

Numerical Modeling of Sediment Transport Processes Caused by Deep Sea Mining Discharges

*J.A. Jankowski*¹

*A. Malcherek*¹

*W. Zielke*¹

¹Institute of Fluid Mechanics, University of Hannover, Appelstr. 9A, D-30167 Hannover, Germany

Abstract - A numerical model was developed in order to estimate the residence time of a sediment plume generated by deep-sea mining activities. The model is capable of simulating density currents in a sediment-laden ocean bottom boundary layer. The numerical model was verified using an analytical solution, which does not take into account the above mentioned effects. The results show that due to density differences the residence time of a plume is reduced substantially.

I. INTRODUCTION

Predictions of the future situation on the raw material market has brought into consideration the commercial exploitation of the mineral deposits located on the seabed. From all of these resources, manganese nodules are of the greatest pragmatic interest because of their nickel, cobalt, copper and manganese contents. The deposits appear in the form of flat horizontal fields on the ocean floor in depths of about 4000–5000 m, with the nodules themselves located directly on the seafloor surface, partially buried or even covered by thin layers of sediments. The deposits and their potential recovery were intensively explored and researched during the last twenty years [1, 2, 3].

There are numerous technical methods available for the mining of these mineral deposits. The most favoured deep-sea mining technology considered in Germany is the use of remotely controlled, self-driving nodule collectors (mining heads) working directly on the sea floor [2, 4]. In order to minimize sediment discharges into the upper ocean zones, the sediment should be directly separated from the nodules by the collector system. After the separation process, the remaining sediment will be introduced into the water column [5]. It will form a plume which can spread with the bottom currents and can - in the worst case - be transported into farther or upper parts of the ocean and form stable turbidity layers. Therefore, one of the problems of the environmental impact assessment of the resuspended sediment is the estimation of its resi-

dence time and distance covered by of the bottom plumes before they eventually dilute approximately to the ambient concentration or deposit at the bottom [6, 7, 8, 9].

Simple estimations of the residence time and the distance which a plume may reach can be based on the assumption of a constant Stokes settling velocity in a uniform velocity field. Such computations for an unfavourable set of parameters can result in residence times of the order of years and transport distances of order of hundreds of kilometers. A more advanced estimation of the plume transport behaviour was developed by [6]. In order to obtain an analytical solution of the sediment transport equation they assumed a constant sediment settling velocity, a uniform flow field over a flat bottom and constant turbulent diffusivities. The complex processes of bottom deposition and erosion are controlled only through one parameter. These assumptions allow the usage of this model for a coarse approximation of the plume spreading. Even in this model an unfavourable set of parameters may lead to very long residence times and distances covered before settling or sufficient dilution of the same order as mentioned above.

The aim of this paper is to analyze the influence of the turbulent characteristics of the bottom boundary layer as well as density currents and stratification induced by the discharged sediment on the residence time of a discharged plume. Therefore, a numerical model for the sediment transport was developed. The analytical solution mentioned above is used to verify the numerical model. The test cases show excellent agreement between analytical and numerical solutions. After validation the numerical model was extended by introducing the bottom boundary layer and density effects. The results for the plume transport behaviour in the near-field change, distinctively reducing the residence time of the plume.

II. NUMERICAL MODEL

A. *The Three-Dimensional Hydrodynamical Model*

The modelling is based on the incompressible Navier-Stokes equations with a free surface boundary condition and the transport equations for tracers, i.e. temperature, salinity, sediment and other needed variables. The algorithm is based on the operator-splitting method. The equations are split into fractional steps with respect to

This work was supported by German Federal Ministry for Science and Technology (BMFT) under Grant No. 03F0010B (Mesoskalige Stofftransporte im Pazifik als Folge des Tiefseebergbaus)

the physical processes and treated by appropriate numerical methods. In the advection part, the method of characteristics is used; the diffusion and free-surface-pressure-continuity steps are treated by finite element methods. The code is fully vectorised using the element-by-element method and takes advantage of the possibilities of modern supercomputers. The code, named TELEMAC-3D, was developed by the Électricité de France [10, 11]. The Institute of Fluid Mechanics participated in the development of the sediment transport model. The hydrodynamic equations to be solved are

$$\begin{aligned} \frac{\partial u}{\partial t} + u \frac{\partial u}{\partial x} + v \frac{\partial u}{\partial y} + w \frac{\partial u}{\partial z} = -\frac{1}{\rho_0} \frac{\partial p}{\partial x} + \frac{\partial}{\partial x} \left(\nu_x \frac{\partial u}{\partial x} \right) \\ + \frac{\partial}{\partial y} \left(\nu_y \frac{\partial u}{\partial y} \right) + \frac{\partial}{\partial z} \left(\nu_z \frac{\partial u}{\partial z} \right) - 2\Omega v \sin \phi \quad (1) \end{aligned}$$

$$\begin{aligned} \frac{\partial v}{\partial t} + u \frac{\partial v}{\partial x} + v \frac{\partial v}{\partial y} + w \frac{\partial v}{\partial z} = -\frac{1}{\rho_0} \frac{\partial p}{\partial y} + \frac{\partial}{\partial x} \left(\nu_x \frac{\partial v}{\partial x} \right) \\ + \frac{\partial}{\partial y} \left(\nu_y \frac{\partial v}{\partial y} \right) + \frac{\partial}{\partial z} \left(\nu_z \frac{\partial v}{\partial z} \right) + 2\Omega u \sin \phi \quad (2) \end{aligned}$$

$$p = \rho_0 g (S - z) + \rho_0 g \int_z^S \frac{\Delta \rho}{\rho_0} dz \quad (3)$$

$$\frac{\partial u}{\partial x} + \frac{\partial v}{\partial y} + \frac{\partial w}{\partial z} = 0 \quad (4)$$

where $\Omega = 2\pi/86164 \text{ s}^{-1}$ is the Earth's angular rotation velocity and ϕ is the latitude.

B. Adjustment to the Deep-Sea Bottom Boundary Layer

The density $\rho = \rho(T, s, p)$ as a function of the temperature T , the salinity s and the pressure p is obtained using the Unesco EOS-80 international equation of state for seawater. The influence of the temperature and salinity on the stratification of the mixed deep-sea bottom boundary layer (BBL) are assumed to be negligible [12]. In this study, which also treats the density currents in the sediment-laden water column, the dependence of the liquid density on the sediment concentration c is assumed to be a linear function:

$$\rho(p, S, T, c) = \rho(p, S, T) + \frac{\rho_{sed} - \rho_0}{\rho_{sed}} c, \quad (5)$$

where $\rho_0 = 999.972 \text{ kg/m}^3$ is the reference density of water at $T_0 = 4^\circ\text{C}$ and ρ_{sed} is the sediment density, assumed to be equal 2560 kg/m^3 . The boundary condition at the bottom is given by the Chezy's formula (τ_b is the bed shear stress):

$$\nu_z \frac{\partial u}{\partial z} = \frac{u \sqrt{u^2 + v^2}}{C^2} = \frac{\tau_b}{\rho} \quad (6)$$

The vertical eddy viscosity and diffusivities are described by a mixing-length model with damping functions ([11]):

$$\nu_z = g(Ri) l^2 \sqrt{\left(\frac{\partial u}{\partial z} \right)^2 + \left(\frac{\partial v}{\partial z} \right)^2} \quad (7)$$

$$\nu_{zT} = f(Ri) l^2 \sqrt{\left(\frac{\partial u}{\partial z} \right)^2 + \left(\frac{\partial v}{\partial z} \right)^2} \quad (8)$$

with the Richardson number

$$Ri = -\frac{g}{\rho} \frac{\frac{\partial \rho}{\partial z}}{\left(\frac{\partial u}{\partial z} \right)^2 + \left(\frac{\partial v}{\partial z} \right)^2} \quad (9)$$

and the mixing length

$$l = \begin{cases} \kappa z & z_f \leq z \leq 0.2\delta \\ 0.2\kappa\delta & 0.2\delta < z \leq \delta \end{cases} \quad (10)$$

where $\kappa = 0.41$ is the von Kármán-constant and z_f the bottom coordinate. The parameter δ controls height of the BBL [13]. The lowest portion of the BBL (approximately between the bottom and 0.2δ) is assumed to be a logarithmic layer (LL) where the velocity is constant in direction and increases in magnitude according to a logarithmic velocity profile. In this model the logarithmic layer is situated in the area, where the mixing length increases linearly. In the rest of the BBL (in the Ekman Layer) the mixing length has a constant value given by (10). Following the above mentioned assumptions, both coefficients δ and C are accordingly calibrated to obtain the velocity profiles in the BBL.

When salinity, sediment or temperature stratification are present, the vertical mixing is damped. This effect is taken into account in (7) and (8) by use of the damping functions $g(Ri)$ and $f(Ri)$, derived from a second-order turbulence model. When the sediment is discharged into a deep-sea boundary layer, the reduced vertical mixing due to the stable stratification has an important influence on the residence time, as it will be shown in the results of this paper.

C. The Sediment Transport Model

The sediment transport equation is given as:

$$\begin{aligned} \frac{\partial c}{\partial t} + u \frac{\partial c}{\partial x} + v \frac{\partial c}{\partial y} + w \frac{\partial c}{\partial z} + \frac{\partial w_c c}{\partial z} = \frac{\partial}{\partial x} \left(\nu_{xc} \frac{\partial c}{\partial x} \right) \\ + \frac{\partial}{\partial y} \left(\nu_{yc} \frac{\partial c}{\partial y} \right) + \frac{\partial}{\partial z} \left(\nu_{zc} \frac{\partial c}{\partial z} \right) \quad (11) \end{aligned}$$

It is solved by splitting this equation into two partial steps: In the advection step only the advective transport

$$\frac{\partial c}{\partial t} + u \frac{\partial c}{\partial x} + v \frac{\partial c}{\partial y} + w \frac{\partial c}{\partial z} = 0 \quad (12)$$

is solved using the method of characteristics. It should be noted that the characteristic curves are already calculated in the hydrodynamic part of the code, so that the advection of sediment requires no further computation costs. In the settling/diffusion step the equation

$$\frac{\partial c}{\partial t} + w_c \frac{\partial c}{\partial z} = \frac{\partial}{\partial x} \left(\nu_{xc} \frac{\partial c}{\partial x} \right) + \frac{\partial}{\partial y} \left(\nu_{yc} \frac{\partial c}{\partial y} \right) + \frac{\partial}{\partial z} \left(\nu_{zc} \frac{\partial c}{\partial z} \right) \quad (13)$$

is treated using finite element method. As initial conditions for this equation the results from the advection step are taken. At the surface, the net sediment flux is zero:

$$\left(w_c \cdot c - \nu_{zc} \frac{\partial c}{\partial z} \right) \Big|_{Surf.} = 0 \quad (14)$$

Erosion and sedimentation at the sediment-water-interface are functions of the bed shear stress τ_b (6), the critical shear stress of deposition τ_{cd} and the critical shear stress of erosion τ_{ce} . If the bed shear stress exceeds the critical deposition shear stress, a particle settled on the bed is immediately resuspended in the flow. If the bed shear stress is less than τ_{ce} , no erosion occurs. The bottom boundary condition can be formulated as follows:

$$\left(w_c \cdot c - \nu_{zc} \frac{\partial c}{\partial z} \right) \Big|_{Bot.} = w_c c |_{Bot.} f_d + M_{res} f_e \quad (15)$$

where the probabilities for deposition and erosion are given by

$$f_d = 1 - \frac{\tau_b}{\tau_{cd}} \quad \text{and} \quad f_e = \frac{\tau_b}{\tau_{ce}} - 1 \quad (16)$$

The resuspension rate M_{res} and the critical stresses τ_{ce} and τ_{cd} must be obtained from empirical formulations. In the following it is assumed that no erosion of the deep-sea bed occurs.

III. VERIFICATION

Usually analytical solutions of the transport equation neglect the complex bottom boundary conditions in connection with the settling velocity because they are obtained from heat transport problems. Lavelle [6] derived an analytical solution for an exponential sediment line source, which also includes erosion and sedimentation such that only the net bottom flux is taken into account. The analytical solution is obtained by assumption of a parallel homogeneous flow in one direction, constant eddy diffusivities and constant settling velocity w_c . As the initial condition an exponential line source is given in the horizontal coordinate origin:

$$c(t) = F_0 e^{-\gamma z} \quad \text{for} \quad x = y = t = 0 \quad (17)$$

This exponential form of the sediment source is believed to be similar to the distribution of the concentration directly nearby the collector (in the radius of ca. 100 m) [6]. The parameters F_0 and γ give the opportunity to control the sediment source. The bottom boundary condition is given as

$$\nu_z \frac{\partial c}{\partial z} - w_c c = \theta c \quad \text{for} \quad z = 0 \quad (18)$$

where θ is defined as adsorptivity index which describes the net flux through the bottom i.e. the difference between the sedimentation and the erosion or resuspension fluxes. It can be concluded, that for $\theta = 0$ there is no net flux through the bottom, whereby for $\theta \rightarrow \infty$ the sediment will immediately be deposited [6, 14]. The solution and the application of this analytical model to the prediction of the deep-sea plumes spreading are described in [6, 15]. As already mentioned, in this model an unfavourable set of parameters may lead to very long residence times and distances covered before settling or sufficient dilution to the ambient concentrations.

A more advanced model, which takes into account not only the set of transport-controlling parameters mentioned above, but also the hydrodynamics of the bottom boundary layer as well as density currents in the sediment-laden water column can lead to different results.

The verification of the sediment transport model of TELEMAC3D involves a test as to whether the sediment transport in the water column as well as the bottom boundary processes are well described. The numerical model should reproduce the analytical solution, when the same assumptions are made. In order to reach the needed similarities, constant eddy diffusivities (also in the vertical direction) for sediment were assumed. The bottom boundary condition was modified in such a manner, that it is equivalent to (18).

In particular this means, that in the equation (15) the probability of erosion f_e (16) was set to zero. Therefore the adsorptivity index could be estimated from

$$\theta = w_c f_d = w_c (1 - \tau_b / \tau_{cd}). \quad (19)$$

As a computational domain, a rectangular area 600×8000 m was chosen. The 2D-mesh covering the area has 572 nodes. The velocity vector is parallel to the longer side of this rectangle, so that there are no fluid fluxes through the side boundaries. The domain, as well as the flow parameters, were chosen in such a way that the suspended sediment cloud will not reach the edges of the domain.

In order to simulate a sediment source at a vertically oriented series of internal nodes of the mesh an exponential distribution of sediment concentration was imposed during the emission time, according to (17). The effective global strength of the source is 10 kg/s, the parameter

for the exponential distribution $\gamma = 0.1 \text{ m}^{-1}$ and the bottom concentration $F_0 = 10 \text{ kg/m}^3$.

Fig. 1 shows a typical numerical result in comparison with the analytical solution. The sediment plume is shown in a vertical section parallel to the velocity and passing through the source position. The source is emitting 48 hours and the plots show the concentration distribution 48h after the emission has stopped. The time step is 3 hours. The settling velocity $w_c = 10^{-4} \text{ m/s}$ with a relatively small absorptivity index ($\theta = 10^{-6} \text{ m/s}$) causes a cumulated cloud in the bottom area. The horizontal and vertical diffusivities are 0.1 and $10^{-3} \text{ m}^2/\text{s}$ respectively. The computed results are in good agreement with the analytical solution.

IV. NUMERICAL STUDIES ON THE SETTLING BEHAVIOUR OF A PLUME IN THE BBL

A parameter study was undertaken with the numerical model. As the bottom of the computational domain a rectangle $4000 \times 2000 \text{ m}$ was taken to allow more diffusive spreading of the plume as in the previous verification case. The domain is discretized using 21 horizontal planes, distributed logarithmically near the bottom and uniformly above. Each plane is discretized using 871 nodes forming 1620 triangular 2D-elements (resolution of 100 m). The assumed water depth is 4000 m.

The results are shown as previously in the form of vertical sections passing through the position of the line source (17) $(x_0, y_0) = (1000, 1000) \text{ m}$ in the direction of the velocity vector, i.e. parallel to the longer edge of the rectangular domain (x -axis). The emission time is 6 h. The area up to 40 m above bottom is shown for $t=12 \text{ h}$, i.e. 6 h after emission stops. To demonstrate the new model features, the dependence of the concentration reduction in the water column associated with the settling velocity is not discussed. Only the case of $w_c = 10^{-4} \text{ m/s}$ is presented, with the deposition probability $f_d = 1$ (100%-probability of deposition) and erosion excluded. The effective strength of the source is taken 1 kg/s and the parameter γ is taken as 0.1 m^{-1} . In order to also illustrate stronger density effects, the case for the strength of 10 kg/s is discussed.

The influence of the Coriolis force is not considered in this study, because the transport time (maximum 12 h) is small when compared with the inertial period $2\pi/f$ at latitudes near the equator (minimum 4 days). Therefore the veering of the velocity vector in the upper portion of the BBL, as well as the influence of the higher frequencies of the current variability are taken into account through the assumption of a greater horizontal sediment diffusivity. As mentioned above, the vertical sediment diffusivities are obtained through the mixing-length model. The constant horizontal values for the sediment are $10^{-4} \text{ m}^2/\text{s}$ in fig. 2 and $1.0 \text{ m}^2/\text{s}$ for fig. 3.

A constant geostrophical velocity of $U_{geo} = 5 \text{ cm/s}$ is

assumed. In the cases, where the bottom friction is taken into consideration, the parameter C for the bottom shear is 200 and $\delta = 10 \text{ m}$ what produces a strongly logarithmic velocity profile in the BBL up to about 2 m. Above 10 m the velocity is U_{geo} .

A plume which does not affect the water density and which spreads in a uniform velocity field is shown in fig. 2a for the smaller horizontal diffusivity case ($10^{-4} \text{ m}^2/\text{s}$). In this case the new features of the numerical model are not included. This figure is shown in order to provide a reference case for the further discussion of the influence of the new parameters controlling the sediment settling.

Fig. 2b shows the case, when the velocity profile in the BBL is taken into account. In the first 4 m above the bottom the transport is reduced, while in the upper parts it is similar to the plume previously presented (fig. 2a). It can also be seen, that the sediment cloud is unstably stratified in the section for $x = 2200 \dots 3700 \text{ m}$. This fact explains the different behaviour of the plume shown in fig. 2c, where density currents and stratification are considered. The unstable stratification shown in fig. 2b induces vertical mixing, which increases the net transport toward the bottom in order to obtain stable stratification. This effect of vertical mixing has a much higher influence on the settling behaviour of the cloud than the sediment settling velocity.

In the case of ten times greater discharge (of 10 kg/s, fig. 2d) these phenomena become more dominant. Due to a stronger emission, greater density gradients cause a horizontal spreading of the plume, which can be counter to the direction of the geostrophical velocity in the lowest portion of the BBL (the position of the source is $x_0=1000 \text{ m}$ and the plume extends upstream to $x=700 \text{ m}$).

The series of plots presented in fig. 3 shows influence of a higher diffusivity of $10 \text{ m}^2/\text{s}$. In the reference case of fig. 3a the concentrations are a few times smaller as in fig. 2a due to a higher horizontal diffusion. In the presence of the BBL (fig. 3b) the concentration and its gradients are also smaller and therefore the density-controlled effects (fig. 3c) are weaker than in the previously discussed less diffusive case.

Nevertheless, when stronger discharge occurs (fig. 3d), the shape of the cloud and the concentrations are only slightly affected by the magnitude of the horizontal diffusivity.

The density induced phenomena, combined with the settling velocity and the fact that the plume shifts practically to the bottom region of the lower ambient velocities, cause a very rapid global settling of the cloud and a tendency to form a flat distribution directly above the bottom. Additionally, the sediment-induced stratification hinders the vertical mixing. This kind of concentration distribution (figures 2d and 3d) provides ideal conditions for a redeposition of the suspended material.

V. REMARKS AND CONCLUSIONS

As the presented parameter study reveals, the behaviour of the discharged plume in a velocity field depends not only on the settling velocity and the diffusion parameters, but also on the velocity structure in the BBL, as well as density currents and stratification.

The near-field effects which control the initial spreading play an important role in the subsequent plume transport. The influence of the velocity profile in the BBL combined with the stratification and the induced mixing effects lead to a substantial reduction of the plume residence time.

The authors believe that flocculation can also be a factor in reducing the residence time. This phenomenon is not considered in this study because no data are available at present. The most important parameters in the flocculation model are the dependency of the settling velocity on the concentration and the turbulent shear stresses.

Future research will concentrate on the development of a mesoscale model of the Peru Basin in the South-East Pacific Ocean with special attention to the bottom boundary layer. This model will include the actual bathymetry as well as the characteristic flow patterns of this region. The verification data for the hydrodynamics are found in [16].

ACKNOWLEDGEMENTS

The research work described in this article is sponsored by the German Federal Ministry for Science and Technology (BMFT) within the interdisciplinary research group TUSCH. The described code TELEMAC3D was developed by the Électricité de France.

REFERENCES

- [1] T. Thijsen, G. Glasby, A. Schmitz-Wiechowski, G. Friedrich, H. Kunzendorf, D. Müller, and H. Richter, "Reconnaissance survey of manganese nodules from the northern sector of the Peru Basin," *Marine Mining*, vol. 2, no. 4, pp. 385–428, 1981.
- [2] H. Kunzendorf, "Proposed marine mineral exploration strategies for the nineties," *Marine Mining*, vol. 7, pp. 233–247, 1988.
- [3] J. Padan, "Commercial recovery of deep seabed manganese nodules: twenty years of accomplishments," *Marine Mining*, vol. 9, pp. 87–103, 1990.
- [4] H. Amann, "The Red Sea Pilot Project: lessons for future ocean mining," *Marine Mining*, vol. 8, no. 1, pp. 1–22, 1989.
- [5] G. Baturin, T. Demidova, K. Y. A., and N. Kurlayev, "The recovery and processing of the iron-manganese nodules and the turbidity of the bottom layer of the ocean," *Oceanology*, vol. 31, no. 4, pp. 473–481, 1991.
- [6] J. Lavelle, E. Ozturgut, S. Swift, and B. Ericson, "Dispersal and resedimentation of the benthic plume from deep-sea mining operations: a model with calibration," *Marine Mining*, vol. 3, no. 1/2, p. 59, 1981.
- [7] J. Lavelle and E. Ozturgut, "Dispersion of deep-sea mining particulates and their effect on light in ocean surface layers," *Marine Mining*, vol. 3, no. 1/2, p. 185, 1981.
- [8] J. Lavelle, E. Ozturgut, E. Baker, and S. Swift, "Discharge and surface plume measurements during manganese nodule mining tests in the North Equatorial Pacific," *Marine Environmental Research*, vol. 7, pp. 51–70, 1982.
- [9] H. Thiel, "From MESEDA to DISCOL: a new approach to deep-sea mining risk assessments," *Marine Mining*, vol. 10, pp. 369–386, 1991.
- [10] J.-C. Galland, N. Goutal, and J.-M. Hervouet, "TELEMAC: A new numerical model for solving shallow water equations," *Adv. Water Resources*, vol. 14, no. 3, pp. 138–148, 1991.
- [11] C. LeNormant, F. Lepage, C. Teisson, A. Malcherek, M. Markofsky, and W. Zielke, "Three dimensional modelling of estuarine processes," in *MAST Days and Euromar Market, Project Reports Volume 1* (K.-G. Barthel, M. Bohle-Carbonell, C. Fragakis, and M. Weydert, eds.), (Brussels), 1993.
- [12] L. Armi and R. C. Millard, Jr., "The bottom boundary layer of the deep ocean," *Journal of Geophysical Research*, vol. 81, pp. 4983–4990, 1976.
- [13] H. Mofjeld and W. Lavelle, "Settling the length scale in a second-order closure model of the unstratified bottom boundary layer," *Journal of Physical Oceanography*, vol. 14, pp. 833–839, 1984.
- [14] I. McCave and S. Swift, "A physical model for the rate of deposition of fine-grained sediments in the deep sea," *Geological Society of America Bulletin*, vol. 87, pp. 541–546, 1976.
- [15] A. Malcherek, J. Jankowski, and H. Hoyme, "SEA-CLOUD: Ein analytisches Modell zur Berechnung des mesoskaligen Stofftransports als Folge des Tiefseebergbaus," report, Institut für Strömungsmechanik und ERiB, Universität Hannover, 1992. (Bericht Nr. AM/003/1992).
- [16] H. Klein, "Near-bottom currents in the deep Peru Basin, DISCOL Experimental Area," *Deutsche Hydrographische Zeitschrift*, 1993. in press.

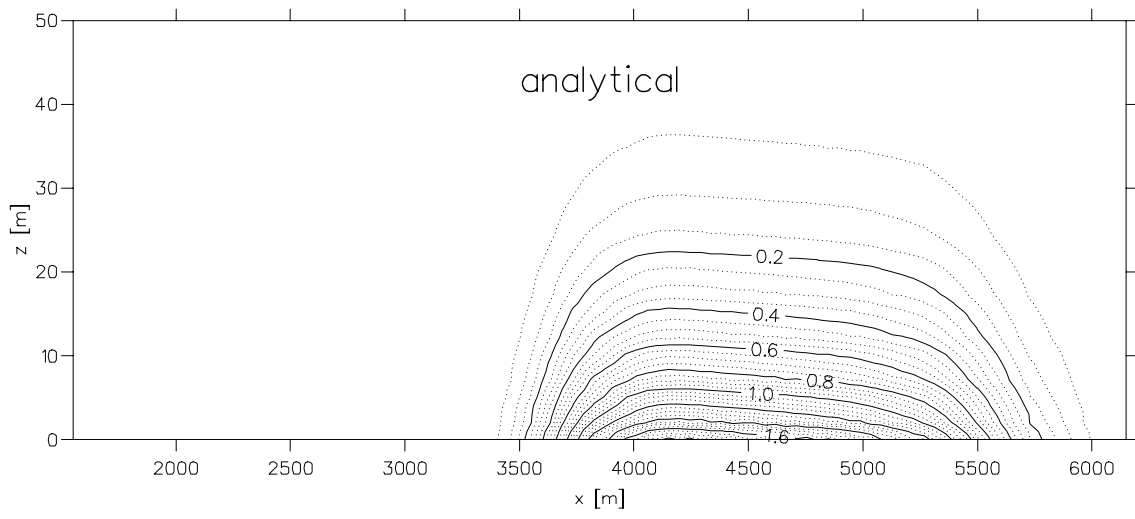
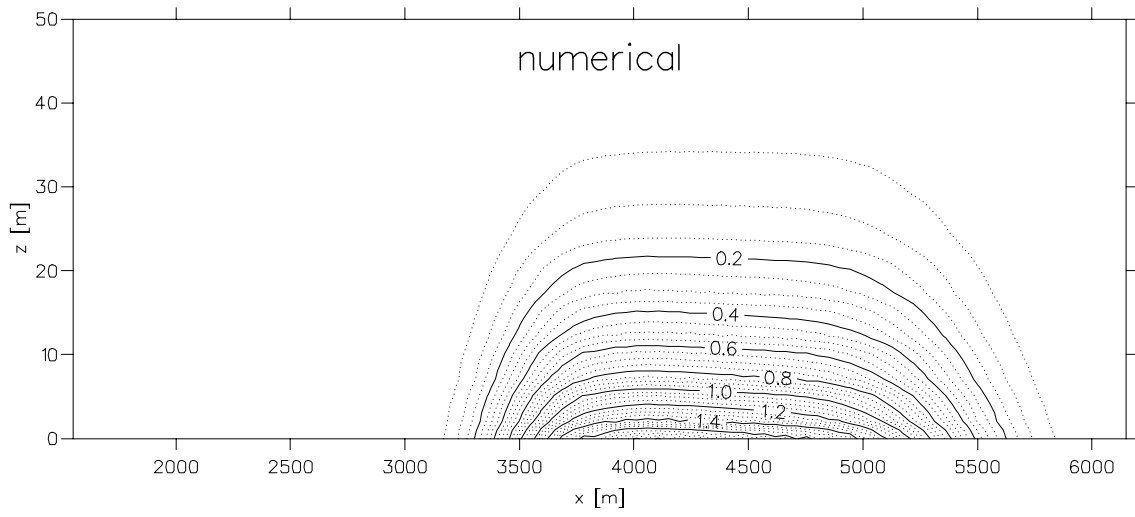


Figure 1. Analytical and numerical solutions. The isoline step is 0.05 g/l.

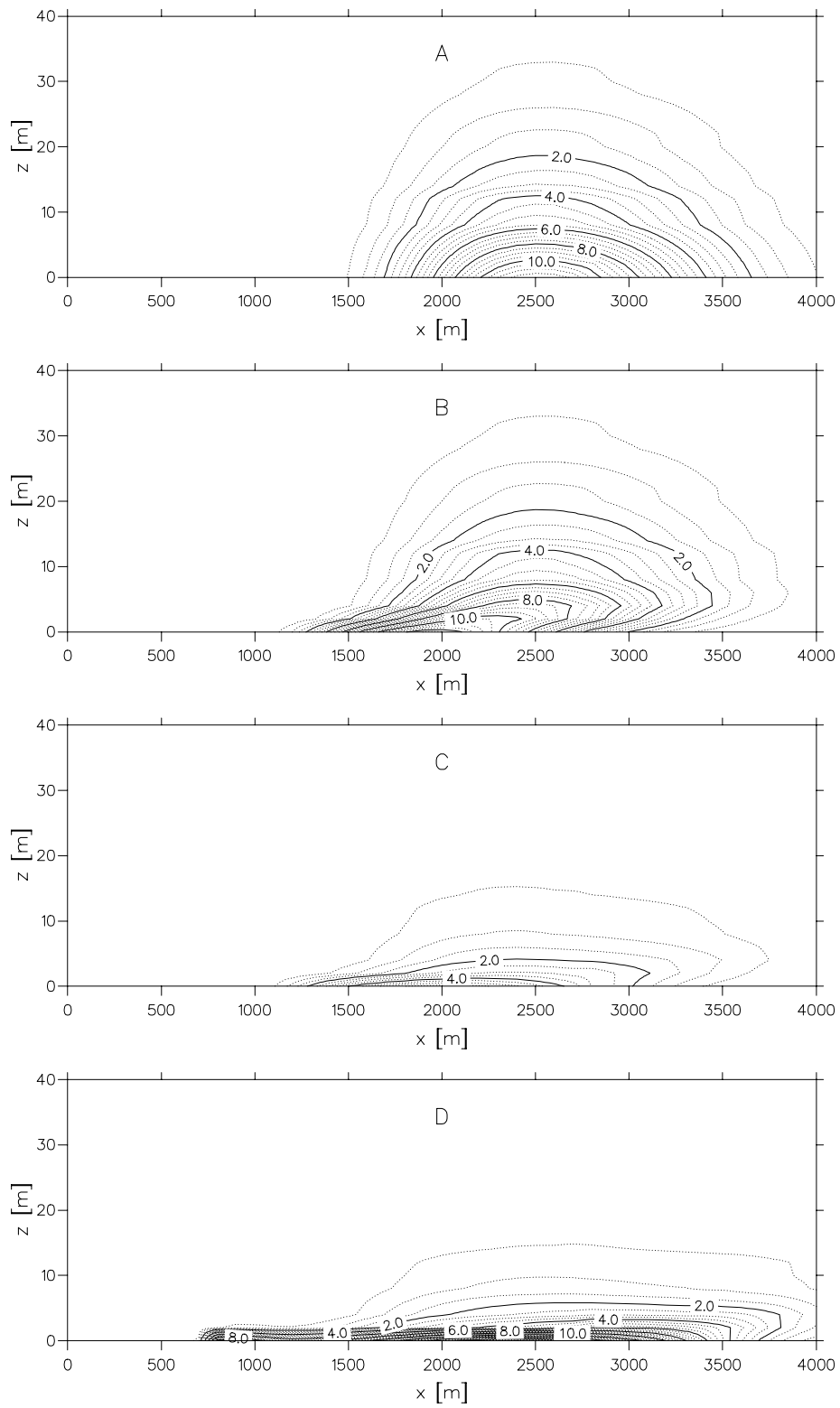


Figure 2. Vertical sections through the sediment plumes in the direction of the current for a low horizontal diffusivity. Description in text. The isoline step is 0.5 mg/l.

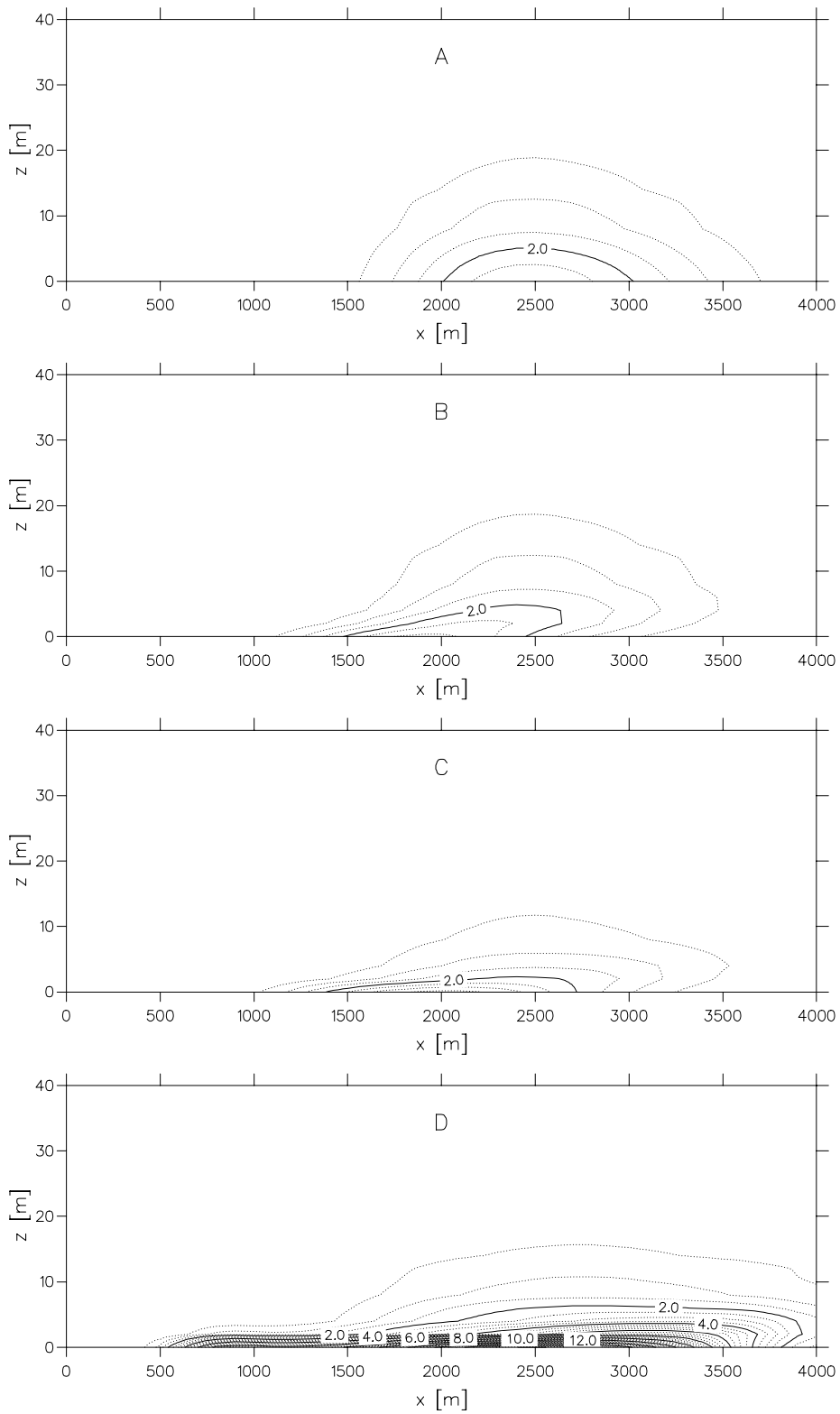


Figure 3. Vertical sections through the sediment plumes in the direction of the current for a higher horizontal diffusivity. Description in text. The isoline step is 0.5 mg/l.